SPECT/CT study of bronchial deposition of inhaled particles in a human aerosol vaccination model against HPV

Vesna Ilic,[1] Vincent Dunet,[1] Alain Le Pape,[2,3] Mikael Buchs,[1] Marek Kosinski,[1] Angelika Bischof Delaloye,[1] Stefan Gerber,[4] John O. Prior[1]

[1]Department of Nuclear Medicine, Lausanne University Hospital, Lausanne, Switzerland; [2]Research Center for Respiratory Diseases, INSERM U1100/EA 6305, François Rabelais University, Tours France; [3]TAAM-CIPA, UPS 44, CNRS, Orléans, France. [4]Gynecology Practice, Fribourg Switzerland

Running Head: SPECT/CT of bronchial deposition

Character count for main text: 19'943 characters (<22'000)

Character count for abstract: 1,777 characters (<1,800)

ENGLISH SUMMARY

Aims—Vaccination by aerosol inhalation can be used to efficiently deliver antigen against HPV to mucosal tissue, which is particularly useful in developing countries (simplicity of administration, costs, no need for cold chain). For optimal immunological response, vaccine particles should preferentially be delivered to proximal bronchial airways. We aimed at quantifying the deposition of inhaled particles in central airways and peripheral lung, and to assess administration biosafety.

Methods—Twenty healthy volunteers (13W/7M, aged 24±4y) performed a 10-min free-breathing inhalation of ^{99m}Tc-stannous chloride colloid aerosol (450 MBq) in a buffer solution without vaccinal particles using an ultrasonic nebulizer (mass median aerodynamic diameter 4.2 μm) and a double mask inside a biosafety cabinet dedicated to assess environmental particle release. SPECT/CT and whole-body planar scintigraphy were acquired to determine whole-body and regional *C/P* distribution ratio (central-to-peripheral pulmonary deposition counts). Using a phantom, SPECT sensitivity was calibrated to obtain absolute pulmonary activity deposited by inhalation.

Results—All participants successfully performed the inhalation that was well tolerated (no change in pulmonary peak expiratory flow rate, $P = 0.9$). It was environmentally safe (no activity released in the biosafety filter.)

1.3±0.6% (range 0.4–2.6%) of the total nebulizer activity was deposited in the lungs with a *C/P* distribution ratio of 0.40±0.20 (range 0.15–1.14).

Conclusion—Quantification and regional distribution of inhaled particles in an aerosolized vaccine model is possible using radioactive particles. This will allow optimizing deposition parameters and determining the particles charge for active-particles vaccination.

ZUSAMMENFASSUNG

Ziel—Die Entwicklung von Aerosol-Impfstoffen mit welchen durch Inhalation Antigene gegen HPV effizient im Schleimhautgewebe aufgenommen werden, könnte in Entwicklungsländern besonders wichtig sein (einfach zu applizieren, kostengünstig, kein Bedarf an Kühlkette, usw.) Um eine optimale immunologische Wirkung zu erzielen, sollte der inhalierte Impfstoff präferentiell in den proximalen Bronchien abgeschieden werden. Das Ziel dieser Studie war es, die Verteilung inhalierter Partikel in den zentralen Bronchien und in peripheren Lungenabschnitten zu messen und deren Biosicherheit zu bestimmen.

Methode—20 gesunde Versuchspersonen (13F/7M, 24±4Jahre) inhalierten während 10 Minuten unter Spontanatmung mittels eines Ultraschall-verneblers (mittlerer aerodynamischer Tröpfchen-Durchmesser 4.2μm) ein Aerosol von ^{99m}Tc-Zinn-Chlorid (450 MBq) in einer Buffer Lösung ohne Impfstoff. Die Inhalation wurde mit einer doppelten Maske in einer speziell dafür entwickelten Abzugshaube durchgeführt und das Austreten von Aerosol-Partikeln in die Umwelt gemessen.

Die Ganzkörper Verteilung und der regionale C/P Verteilungskoeffizient (Quotient zentrale über periphere Lungenaktivität) wurden mittels der SPECT/CT und einer Ganzkörper-Szintigraphie bestimmt. Die SPECT

Empfindlichkeit wurde mittels eines Phantoms kalibriert, um die absolute inhalierte Aktivität in der Lunge zu bestimmen.

Ergebnisse—Die Inhalation wurde von allen Studienteilnehmern vollendet und gut vertragen (Peak Flow unverändert, *P*=0.9). Der Biosicherheitsfilter war frei von Radioaktivität. 1.3±0.6% (0.4–2.6%) der Gesamtaktivität des Verneblers wurde in den Lungen gemessen, mit einem C/P Verteilungsquotienten von 0.40±0.20 (0.15–1.14).

Schlussfolgerung—Die Aufnahme und regionale Verteilung inhalierter Partikel können in einem Aerosol-Impf-Modell mittels radioaktiv markierter Partikel quantitativ bestimmte werden und so zur Optimierung der Parameter beitragen, die für Verteilung und Beladung von aktiven Impfstoff-Partikeln von Bedeutung sind.

SCHLÜSSELWÖRTER

CORRESPONDING AUTHOR:

Prof. John O. Prior, PhD MD

Department of Nuclear Medicine and Molecular Imaging

Lausanne University Hospital

Rue du Bugnon 46. 1011 Lausanne. Switzerland

Tel. +41 21 314 43 48, Fax +41 21 314 43 49

john.prior@chuv.ch

INTRODUCTION

Vaccines constitute one of the most cost-effective preventive measures against illness and death from infectious disease [23]. Each year, five million people die worldwide from mucosally transmitted diseases that might be prevented by vaccines [8]. Cervical cancer is the second most common cancer in women in the world, the most common in Africa and the leading cause of cancer deaths in developing countries [4]. Vaccines against the leading HPV oncogenic types 16 and 18 are available with efficacy exceeding 95% in HPV-uninfected women [37]. However, efficient vaccination programs are difficult to implement in developing countries mainly because of currently prohibitive costs.

Despite the unprecedented medical success of vaccination, traditional application routes (intramuscular or subcutaneous) are not without limitations. In the context of mass vaccination campaigns in developing countries, needle-free vaccination can increase compliance (reduced local pain and side effects) and decrease overall costs (no need for needle disposal, etc.) Specific vaccine formulations abolish the need for a "cold chain" (specific equipment, and procedures to maintain vaccine at low temperatures until administration) [19,24,28] and aerosol immunization is such an alternative. This is offering many advantages: ease of application by paramedical personnel, lesser invasiveness favouring acceptance, reduced risk of cross-contamination by blood-born infectious agents, diminished

medical waste, and lower costs thanks to the use of multidose vials, among others [2,21]. Moreover, aerosol vaccination may induce better immunogenicity than conventional subcutaneous injections [8] because mucosal immune response might induce broader protection due to the production of IgA in addition to systemic IgG antibodies [30,39].

Nuclear medicine is a unique resource for the translational research about therapies delivered as aerosols. Indeed, for both research and development SPECT or PET of aerosol lung deposition is the most relevant strategy to pre-clinically assess the actual dose delivered to the target area [7,9,15]. At the time of translation to clinical trials, lung deposition imaging allows to optimize aerosol delivery to the target for immunization (central lung) while minimizing potential side effects due to deposition in less effective area (peripheral lung).

In a preclinical validation study in non-human primates, Corbett *et al.* [8] showed that aerosol-delivered poxvirus-based vaccination was safe, feasible, and immunogenic. The next step towards clinical implementation consists in validating this aerosol vaccination in humans. However, before dose escalation and safety analysis of side effects, more information needs to be collected about vaccinal particle charge and lung distribution during the face-mask aerosol nebulization [39]. Thus, the aims of our study were: (1) to assess the fraction of the nebulized particles delivered to the lungs to decide about the future viral charge; (2) to demonstrate a privileged

deposition of aerosolized particles into the central part of the lungs to elicit optimal immunological response, while limiting the alveolar exposure (not essential to proper immunization) and potential inflammation; and (3) to verify administration safety by quantifying environmental particle release.

METHODS

Study population

Healthy volunteers were prospectively recruited by advertisement at the Lausanne University Hospital, Switzerland. Before inclusion, they underwent history taking (personal medical history including pulmonary disease, infectious disease, smoking, asthma and chronic obstructive pulmonary disease) and a physical examination. Peak expiratory flow rate (PEFR) was measured immediately before and after inhalation as a simple surrogate for asthma detection and to detect any subclinical change due to the aerosol-induced broncho-constrictive reaction. Women of childbearing age underwent a pregnancy test; a negative result was required before inclusion. The Local Ethic Committee, the Swiss Federal Office of Public Health and Swissmedic approved the study protocol and participants signed a written informed consent form. Participants received a total effective dose of 1.9 mSv (1.0 mSv from the radiotracer and 0.9 mSv for the low-dose/slow-rotating CT) [36]. The radiation effective dose was obtained by

assuming that a maximum of 17% of the nebulized activity would be distributed in the patient based on a preclinical study [26] and an effective dose ED of 0.014 mSv/MBq computed from known organ distribution of nanocolloid aerosol (Venticoll™, GE Healthcare Srl, Milano, Italy) and ICRP 60 tissue weighting factors.

Radiolabeling of particles and nebulization procedure

The deposition procedure used non-viral, inert stannous chloride particles (MTcK-2, Polatom, Otwork-Świerk, Poland) labeled with [99mTc], with >90% of particles sized within 459–1110 nm (peaking at 788 nm) dispersed in a 4-mL buffer solution of identical physical and chemical characteristics as the future vaccine but without immunogenic, sub-micrometric particles (Tris buffer 1.2g/L, saccharose 50g/L, Na glutamate 1.87g/L, NaCl 2.9 g/L, titrated with 5N HCl for pH 8.0). As previously described [26], aerosol generated from such a formulation exhibits the same granulometry and lung deposition pattern as the vaccine due to the low protein content. Labeling was performed according to the manufacturer instructions [34]. Preliminary measurements were conducted to verify labeling and particle size stability in the buffer solution (pH 8) during nebulization (data not shown).

An ultrasonic nebulizer (Atomisor Megahertz AMGH, La Diffusion Technique, St-Etienne, France) was used to create aerosol from radiolabeled solution. Using a nebulization power set at 10/10, a 4.2 µm mass median

aerodynamic diameter (MMAD) aerosol was generated to favour central pulmonary distribution with care to prevent any temperature increase during sonication. To further privilege central pulmonary distribution of the aerosol, we chose active inhalation with disconnected internal ventilator and set tubing lengths 1 and 2 to get 75- and 300-ml buffer volumes, respectively (**Figure 1A**). For the inhalation process, the subject was placed in front of a biosafety cabinet containing a class-E12 HEPA filter, and equipped with a Double Mask system (Medicvent, Umeå, Sweden). The soft inner mask was connected to the nebulizer chamber and the hard outer mask evacuation outlet was connected to the biosafety cabinet aspiration through a separate HEPA filter to trap any aerosol particle escaping from the inner mask. The participants were instructed to freely inhale the nebulized aerosol in a controlled and reproducible tidal breathing manner for 10 minutes [27]. Residual activity in the nebulizer reservoir and tubing system was measured before and after the aerosol delivery. The activity released in the environment from the nebulization procedure was aspirated through the biosafety cabinet HEPA filter, whose activity was measured distant from the participant outside the administration room.

Imaging acquisition and processing

Twenty minutes after inhalation every participant underwent a SPECT/CT acquisition (Hawkeye IV, GE Healthcare, Milwaukee, MI) using an energy

window 140 keV±20%, 60 projections of 8 sec, a 128x128 matrix, and CT acquisition parameters: 140kV, 2.5mA, helical, pitch 1.5, slice thickness 5mm. Participants also underwent a whole-body planar scintigraphy in both anterior and posterior view 50 min post inhalation (scan velocity 10cm/min, 256×1024 pixel).

Raw data were processed on a dedicated workstation (Xeleris 3, GE Healthcare, Milwaukee, MI) by two experienced nuclear medicine physicians, in consensus. SPECT/CT images were reconstructed using 2D-OSEM (10th-order Butterworth, 0.5-cycle/cm cut-off frequency). Regions of interest (ROI) were drawn on whole-body anterior and posterior images around each lung and for the whole-body; counts were computed using geometrical mean. On tomographic images, volumes of interest (VOI) were drawn following anatomical boundaries provided by CT on separate transaxial slices centered on the hilum for 1-st order bronchi and applied to the reconstructed SPECT dataset. This allowed to separate central particle deposition (from carina to lobar bronchus division) from peripheral deposition (beyond lobar bronchus division) (**Figure 3 A**) and to compute the central-peripheral deposition ratio $C/P = COUNTS_{central}$ / $COUNTS_{peripheral}$. A semi-quantitative analysis to compute a scintigraphic C/P index was also performed to quantify the uptake in central bronchi as compared to pulmonary parenchyma on the SPECT transaxial slices using a 5-point Likert scale: C/P index = grade 0: no difference; grade 1:

questionable difference; grade 2: faint difference; grade 3: marked

difference; grade 4: very strong difference.

For quantifying total pulmonary particle deposition *TPD*, the

sensitivity of SPECT/CT was calibrated using a 200-mL reference phantom

containing 5MBq of $^{99\mathrm{m}}$Tc-pertechnetate imaged using the same SPECT

acquisition and reconstruction parameters. This allowed computing the

activity deposited in the lung volume from the total counts. The percentage

of nebulized activity deposited in the lungs was then computed as *TPD* (%)

$= 100 \cdot COUNTS_{\mathrm{lungs}}$ / $COUNTS_{\mathrm{standard}} \cdot 5$ (MBq) / $Activity_{\mathrm{nebulizer}}$ (MBq).

Then, the absolute central pulmonary deposition *CPD* can be derived as

$CPD = TPD \cdot [C/P]$ / $(1 + [C/P])$. All measured activities were corrected for

the physical half-life of $^{99\mathrm{m}}$Tc.

Statistical analysis

Continuous variables are presented as *mean±SD* or as *median* and 25th to

75th percentile *interquartile range* (IQR), and categorical variables are

presented as number and percentage. We used non-parametric Wilcoxon

rank sum test to compare continuous variables before and after the exam as

well as to compare variables according to gender and smoking status.

Association between variables was assessed using non-parametric Spearman

correlation coefficient (ρ). Statistical analyses were performed with Stata

12.1 software (Stata Corp., College Station, TX) and a *P*-value <0.05 was considered as statistically significant.

RESULTS

Population

Twenty-one healthy volunteers were enrolled and complete data were available in twenty participants (13 women, 7 men) aged 24±4 years. None had history of asthma or any other chronic or recent pulmonary condition; 5 were smokers (25%). Pulmonary auscultation was unremarkable in all participants and peak expiratory flow rate was within normal range for age and sex (**Table 1**).

Inhalation and procedure safety

The 10.0-min nebulization could be performed safely in all participants with an activity of 430±20 MBq of ^{99m}Tc-colloid introduced in the nebulizer chamber. No participant experienced dyspnea during or after inhalation. No unexpected side effects or coughing were observed. Peak expiratory flow rate at the end of the study was identical to baseline ($P = 0.9$), also in subgroup analyses by gender and smoking status (**Tab. 1**). As expected, PEFR was significantly related to participants' gender (–28% in women), height ($\rho =0.78$, $P=0.0002$) and body surface area ($\rho =0.69$, $P=0.001$).

The nebulization was also safe for the environment; no activity was released from the nebulization system or from the double mask in the biosafety cabinet HEPA filter. At the end of the inhalation, the nebulization system contained >90% of the activity, with the largest activity in the nebulization chamber (**Fig. 1A and 1B**).

Inhaled particle distribution

Whole-body scans revealed that inhaled particles were mainly localized in respiratory and digestive tracts, *i.e.* the mouth/oropharynx ($N = 20$), esophagus ($N = 9$), stomach ($N = 17$) and bowel ($N = 13$) due to saliva swallowing (**Figure 1C**). Of note, minimal activity could be seen in the bladder ($N = 2$, different than the one of Figure 1) and no activity was seen in the liver, spleen, kidney, thyroid or bone marrow.

On planar scintigraphy, lung activity represented 40±9% of the total whole-body activity. There was no difference according to gender (women 38±8% vs. men 43±11%, P=0.4) or to smoking status (non-smokers 39±10% vs. smokers 43±6%, $P = 0.2$). On SPECT images, 54±4% particles were localized in the right lung and 46±4% in the left lung ($P < 0.0001$). This relative distribution was neither influenced by gender ($P = 0.7$) nor by smoking status ($P = 0.6$). There was also no significant difference between upper, middle and lower third of lung fields ($P > 0.6$).

Total pulmonary deposition, *TPD* was 1.3±0.6% (range 0.4–2.6%) of the total activity initially present in the nebulizer (**Fig. 2**). Residual inhaled particles were also seen on SPECT/CT in the trachea ($N = 13$) and on the skin ($N = 9$) due to salivary contamination from the mouth after inhalation. There was no significant difference between men and women (1.4±0.7% vs. 1.2±0.6%, $P = 0.9$) or between smokers and non-smokers (1.4±0.7% vs. 1.2±0.6%, $P = 0.7$).

Regional lung distribution of inhaled particles

SPECT/CT showed a central to peripheral deposition ratio *C/P* of 0.4±0.2 (range 0.15–1.14) and a central pulmonary deposition *CPD* of 0.3±0.3% (range 0.1–1.4) (**Fig. 2**). An example is illustrated in **Fig. 3**, with VOI drawn for computing the central and peripheral activity. The *C/P* ratio was not affected by the smoking status (non-smokers 0.36±0.11 vs. smokers 0.51±0.36, $P = 0.6$), but tended to be higher for women than men (0.46±0.22 vs. 0.30±0.11, $P = 0.06$). Of note, *C/P* ratio was significantly correlated with PEFR ($\rho = -0.58$, $P = 0.01$).

The semi-quantitative C/P index showed a favourable central distribution with 11/20 (55%) of the participants showing a marked or very strong uptake and 15/20 (75%) showing a higher uptake in central regions than in parenchyma (grade 2 or above) (**Fig. 4**).

DISCUSSION

Thanks to the use of scintigraphic imaging to optimize the deposition within the central lung, preclinical studies of aerosol administration poxvirus-based vaccines in non-human primates have led to a safe and long-lasting immune response [8,26]. Here, we performed a proof-of-concept study in volunteers to assess the feasibility of aerosol nebulization, including the basic safety profile of non-vaccinal buffer solution at the individual and environmental level, and to quantify regional distribution. Our results demonstrate that quantification of the regional distribution of radiolabeled aerosols in a human vaccine model without immunogenic particles is feasible. Moreover, the administration is safe for the participants and the environment. These results are encouraging for future vaccine application trials in humans, where the full safety profile and immune response will be assessed.

Within the lung, several factors may influence the site of particle deposition, the size being one of the most important [18]. Particle sizes of 4–5μm, such as the one produced in our study are thought to be optimal for a central deposition of an aerosol in the lungs [5]. The central lung is considered as the target area to elicit optimal immunological response [1,3,8,29,33]. The human upper airway mucosa contains a dense network of antigen-presenting cells throughout the nasal cavity, trachea, and lungs ready to initiate immune response when in contact with a microbial burden

[20]. During inspiration, larger particles will be deposited merely in the tubing system and smaller ones in the peripheral part of the lung [2,6,10].

Planar gamma camera scintigraphy is well established for measuring deposition of radioaerosols [11,38]. SPECT /CT provides 3-dimensional, detailed information and offers a superior assessment of aerosol deposition [13,14,16]. In addition, we performed CT-based attenuation corrections of the SPECT images and used a calibration factor derived from a phantom to more accurately assess the activity deposited in target regions [27]. Our results support the feasibility of aerosol delivery of vaccines with preferred central lung distribution, in agreement with previous results in a series of 8 non-human primates [8].

The efficacy of inhaled drugs, whether given for treatment of lung disease [17,25,32,35] or to achieve an effect in some other part of the body, depends on drug deposition in the lungs. Our results with mean lung deposition *TPD* of 1.3±0.6% of the total nebulized activity were within range of values observed in the preclinical non-human primate study (3.6±1.1% and 1.8±0.5% for two different strains of poxvirus-based vaccine) [8]. Although this figure may seem low, it was sufficient to elicit durable vaccine immune response [8]. Similarly, our central-to-peripheral deposition ratio reached 0.4±0.2, close to the non-human primate preclinical values (*C/P* = 0.75 in average) [8] and is in agreement with our previsions in order to limit exposure of alveoli to vaccinal proteins

considering a potential risk of alveolitis. It is true that ultrafine aerosol-like deposition can reach up to 30% in a single-breath, but with a clearly alveolar distribution, which is not what is needed for the same reason (eventual risk of alveolitis). For the first clinical studies, these safety considerations have oriented our choice on this particular ultrasonic nebulizer despite a relatively low predicted efficiency for delivering the aerosol to the central airways. Following this modelization study, this device will allow to precisely deliver escalating doses for the assessment of both efficacy and safety of the vaccine.

A few limitations to our study need to be mentioned. This study was performed in healthy participants. However, in patients with airway disease, aerosol deposition can be different, namely with a more pronounced central deposition and a potentially faster washout of centrally deposited aerosols by mucociliary clearance or cough reflex [12]. However, this should not be a major problem in the proposed HPV vaccine model, as potential subjects would be young, non-HPV-exposed and devoid of lung disease. It is also worth mentioning that non-human primates were pre-treated with atropine not only to reduce salivation, but also to get transient inhibition of the bronchial mucociliary clearance and favour antigen presentation; thus, the effect of mucociliary clearance or its transient inhibition need obviously to be specifically studied. This was not done in this study on volunteers and could have influenced the results. Moreover,

non-human primate results were also developed using planar scintigraphy and there are known differences between regional pulmonary depositions measured on 2-D planar scans and 3-D SPECT [14]. Finally, the assessment of nebulized particles could also be performed by PET with several advantages over SPECT (absolute quantitation without the need of a calibration standard, shorter isotope half-life) [31] but the labelling of aerosols with positron emitters remains challenging. $^{13}NH_2$ has been employed to image saline-based aerosols but requires an on-site cyclotron[40]. Of note, the availability of $^{68}Ge/^{68}Ga$ generators may facilitate the use of PET in aerosol deposition research in the future with the possibility to directly use ^{68}Ga instead of ^{99m}Tc to label kit-based radiopharmaceuticals [22].

In conclusion, we demonstrated a feasible and safe method for aerosol delivery in humans of non-viral inert particles with identical physical and chemical characteristics as the future vaccine. Our study provides a bridge between in vivo preclinical testing and clinical trials, allowing the latter to be planned with increased confidence. The present work emphasizes the unique contribution of nuclear imaging in translational research for pulmonary delivery of active formulations administered as aerosols. Further studies will be needed to determine the optimal viral charge needed to guarantee the appropriate dose of active particles

deposited in the immunogenic central area and assess the immune response of aerosol vaccine.

DISCLOSURE STATEMENT

The authors declare that they have no conflict of interest.

REFERENCES

1. Balmelli C, Roden R, Potts A, et al. Nasal immunization of mice with human papillomavirus type 16 virus-like particles elicits neutralizing antibodies in mucosal secretions. J Virol 1998; 72: 8220-8229

2. Bennett WD, Brown JS, Zeman KL, et al. Targeting delivery of aerosols to different lung regions. J Aerosol Med 2002; 15: 179-188

3. Bergquist C, Johansson EL, Lagergard T, Holmgren J, Rudin A. Intranasal vaccination of humans with recombinant cholera toxin B subunit induces systemic and local antibody responses in the upper respiratory tract and the vagina. Infect Immun 1997; 65: 2676-2684

4. Bosch FX, Lorincz A, Munoz N, Meijer CJ, Shah KV. The causal relation between human papillomavirus and cervical cancer. J Clin Pathol 2002; 55: 244-265

5. Brown JS, Zeman KL, Bennett WD. Regional deposition of coarse particles and ventilation distribution in healthy subjects and patients with cystic fibrosis. J Aerosol Med 2001; 14: 443-454

6. Conway J. Lung imaging - two dimensional gamma scintigraphy, SPECT, CT and PET. Adv Drug Deliv Rev 2012; 64: 357-368

7. Conway J, Fleming J, Bennett M, Havelock T. The co-imaging of gamma camera measurements of aerosol deposition and respiratory anatomy. J Aerosol Med Pulm Drug Deliv 2013; 26: 123-130

8. Corbett M, Bogers WM, Heeney JL, et al. Aerosol immunization with NYVAC and MVA vectored vaccines is safe, simple, and immunogenic. Proc Natl Acad Sci U S A 2008; 105: 2046-2051

9. Corcoran TE. Imaging in Aerosol Medicine. Respir Care 2015; 60: 850-855; discussion 855-857

10. Dijk PH, Heikamp A, Piers DA, Weller E, Bambang Oetomo S. Surfactant nebulisation: safety, efficiency and influence on surface lowering properties and biochemical composition. Intensive Care Med 1997; 23: 456-462

11. Dolovich MB. Measuring total and regional lung deposition using inhaled radiotracers. J Aerosol Med 2001; 14 Suppl 1: S35-44

12. Eberl S, Chan HK, Daviskas E, Constable C, Young I. Aerosol deposition and clearance measurement: a novel technique using dynamic SPET. Eur J Nucl Med 2001; 28: 1365-1372

13. Eberl S, Chan HK, Daviskas E. SPECT Imaging for Radioaerosol Deposition and Clearance Studies. J Aerosol Med 2006; 19: 8-20

14. Fleming J, Conway J, Majoral C, et al. The use of combined single photon emission computed tomography and X-ray computed tomography to assess the fate of inhaled aerosol. J Aerosol Med Pulm Drug Deliv 2011; 24: 49-60

15. Fleming J, Conway J, Majoral C, et al. Controlled, Parametric, Individualized, 2-D and 3-D Imaging Measurements of Aerosol

Deposition in the Respiratory Tract of Asthmatic Human Subjects for
Model Validation. J Aerosol Med Pulm Drug Deliv 2015; 28: 432-451

16. Fleming JS, Epps BP, Conway JH, Martonen TB. Comparison of
SPECT aerosol deposition data with a human respiratory tract model. J
Aerosol Med 2006; 19: 268-278

17. Gagnadoux F, Hureaux J, Vecellio L, et al. Aerosolized chemotherapy.
J Aerosol Med Pulm Drug Deliv 2008; 21: 61-70

18. Gajdocsi R, Bikov A, Antus B, et al. Assessment of reproducibility of
exhaled hydrogen peroxide concentration and the effect of breathing
pattern in healthy subjects. J Aerosol Med Pulm Drug Deliv 2011; 24:
271-275

19. Giudice EL, Campbell JD. Needle-free vaccine delivery. Adv Drug
Deliv Rev 2006; 58: 68-89

20. Jahnsen FL, Gran E, Haye R, Brandtzaeg P. Human nasal mucosa
contains antigen-presenting cells of strikingly different functional
phenotypes. Am J Respir Cell Mol Biol 2004; 30: 31-37

21. Jia Y, Krishnan L, Omri A. Nasal and pulmonary vaccine delivery
using particulate carriers. Expert Opin Drug Deliv 2015; 12: 993-1008

22. Kotzerke J, Andreeff M, Wunderlich G, Wiggermann P, Zophel K.
[Ventilation-perfusion-lungscintigraphy using PET and 68Ga-labeled
radiopharmaceuticals]. Nuklearmedizin 2010; 49: 203-208

23. Koutsky LA, Ault KA, Wheeler CM, et al. A controlled trial of a human papillomavirus type 16 vaccine. N Engl J Med 2002; 347: 1645-1651

24. Laube BL. The expanding role of aerosols in systemic drug delivery, gene therapy and vaccination: an update. Transl Respir Med 2014; 2: 3

25. Lemarie E, Vecellio L, Hureaux J, et al. Aerosolized gemcitabine in patients with carcinoma of the lung: feasibility and safety study. J Aerosol Med Pulm Drug Deliv 2011; 24: 261-270

26. Lerondel S, Le Pape A, Sene C, et al. Radioisotopic imaging allows optimization of adenovirus lung deposition for cystic fibrosis gene therapy. Hum Gene Ther 2001; 12: 1-11

27. Lerondel S, Vecellio None L, Faure L, et al. Gene therapy for cystic fibrosis with aerosolized adenovirus-CFTR: characterization of the aerosol and scintigraphic determination of lung deposition in baboons. J Aerosol Med 2001; 14: 95-105

28. Levine MM. Can needle-free administration of vaccines become the norm in global immunization? Nat Med 2003; 9: 99-103

29. Nardelli-Haefliger D, Roden RB, Benyacoub J, et al. Human papillomavirus type 16 virus-like particles expressed in attenuated Salmonella typhimurium elicit mucosal and systemic neutralizing antibodies in mice. Infect Immun 1997; 65: 3328-3336

30. Nardelli-Haefliger D, Lurati F, Wirthner D, et al. Immune responses induced by lower airway mucosal immunisation with a human papillomavirus type 16 virus-like particle vaccine. Vaccine 2005; 23: 3634-3641

31. Newman S, Fleming J. Challenges in assessing regional distribution of inhaled drug in the human lungs. Expert Opin Drug Deliv 2011; 8: 841-855

32. Newman SP, Sutton DJ, Segarra R, Lamarca R, de Miquel G. Lung deposition of aclidinium bromide from Genuair, a multidose dry powder inhaler. Respiration 2009; 78: 322-328

33. Ogra PL, Faden H, Welliver RC. Vaccination strategies for mucosal immune responses. Clin Microbiol Rev 2001; 14: 430-445

34. Polatom. Kit for the preparation of 99mTc-Colloid. 2009

35. Sangwan S, Agosti JM, Bauer LA, et al. Aerosolized protein delivery in asthma: gamma camera analysis of regional deposition and perfusion. J Aerosol Med 2001; 14: 185-195

36. Sawyer LJ, Starritt HC, Hiscock SC, Evans MJ. Effective doses to patients from CT acquisitions on the GE Infinia Hawkeye: a comparison of calculation methods. Nucl Med Commun 2008; 29: 144-149

37. Sitas F, Parkin DM, Chirenje M, et al. Part II: Cancer in Indigenous Africans--causes and control. Lancet Oncol 2008; 9: 786-795

38. Snell NJ, Ganderton D. Assessing lung deposition of inhaled medications. Consensus statement from a workshop of the British Association for Lung Research, held at the Institute of Biology, London, U.K. on 17 April 1998. Respir Med 1999; 93: 123-133

39. Tonnis WF, Lexmond AJ, Frijlink HW, de Boer AH, Hinrichs WL. Devices and formulations for pulmonary vaccination. Expert Opin Drug Deliv 2013; 10: 1383-1397

40. Venegas J, Winkler T, Harris RS. Lung physiology and aerosol deposition imaged with positron emission tomography. J Aerosol Med Pulm Drug Deliv 2013; 26: 1-8

FIGURES LEGENDS

Fig. 1. Distribution of the radiolabelled particles after nebulization. (**A**) Nebulization system (f = filter, m = mask; nc = nebulization chamber; 1 = 75-mL tubing; 2 = 300-mL tubing; *connected together during operation). (**B**) Corresponding planar scintigraphy of nebulization system. (**C**). Anterior and posterior whole-body planar scintigraphy showing particle distribution in the lung and mouth, oropharynx, trachea and stomach (s), but not in the thyroid, kidney, bladder, liver or spleen.
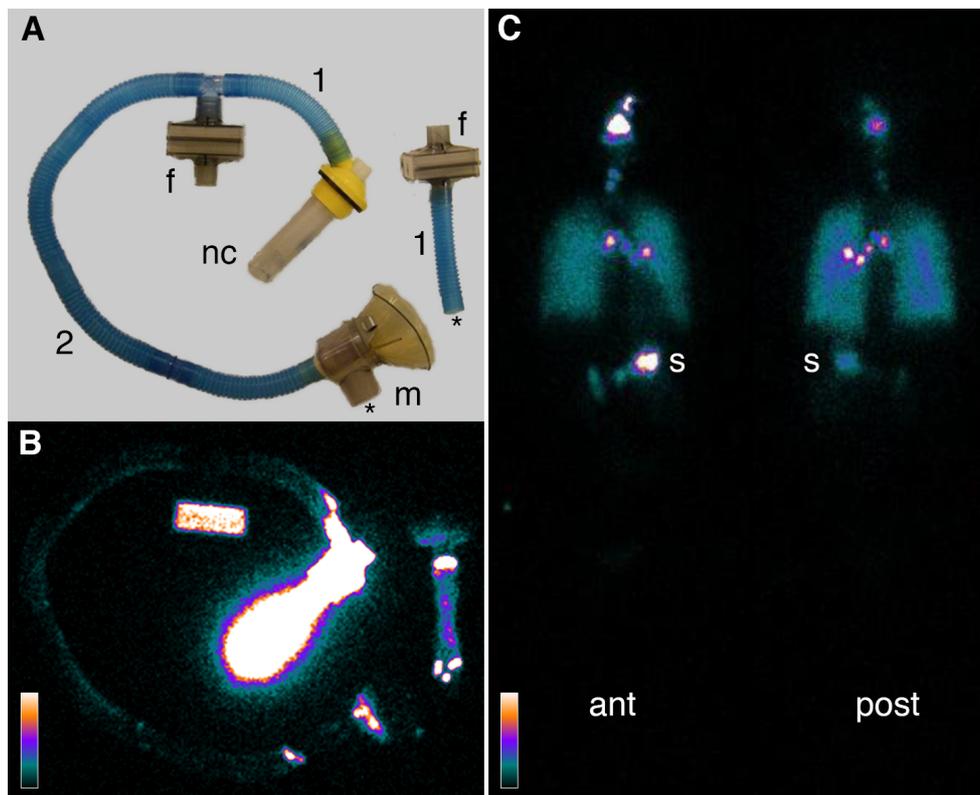
Fig. 2. Boxplot of the total pulmonary deposition (*TPD*), central pulmonary deposition (*CPD*) and central-to-peripheral distribution ratio (*C/P*) (*N* = 20). Boxes represent the limits of the 1st and 3rd quartiles, as well as the median; numbers represent the *mean* [*95%CI*]
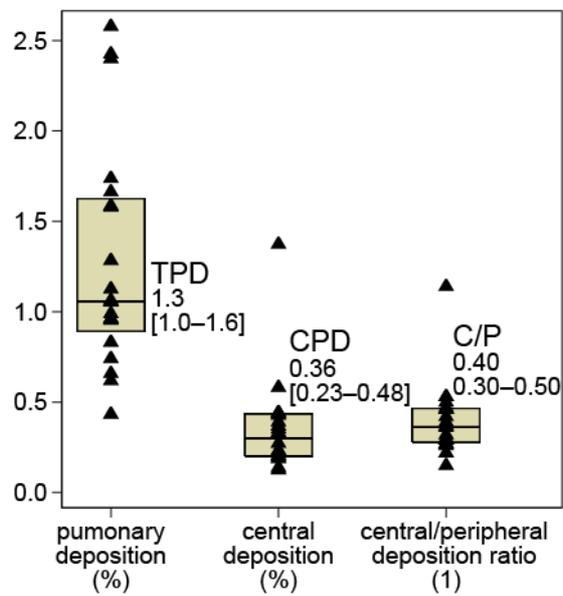
Fig. 3. SPECT/CT imaging of particles deposition in the lung. (**A**) SPECT (*first row*) and SPECT/CT fusion (*second row*) images showing excellent central deposition. (**B**) Maximum intensity SPECT projection in anterior view. (**C**) Three-dimensional image rendering fusion of the airways on CT and SPECT activity showing central bronchial accumulation of inhaled particles.
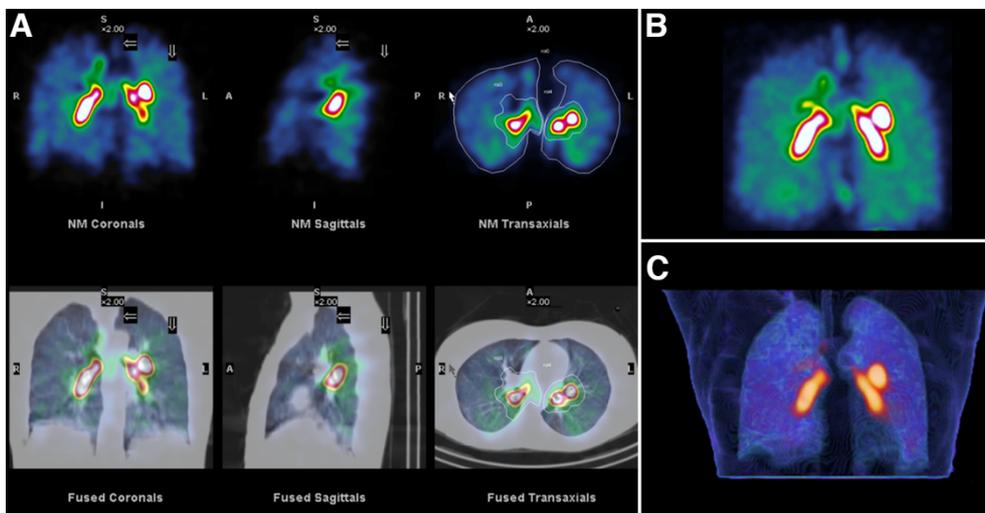
Fig. 4. Scintigraphic index of central/peripheral distribution of inhaled particles. This histogram shows the best side's uptake in central bronchi as compared to pulmonary parenchyma uptake on SPECT with an example of anterior view of the maximum intensity projection image for each class (grade 0 = no difference; grade 1 = doubtful difference; grade 2 = faint difference; grade 3 = marked difference; grade 4= very strong difference). In total, 75% of the participants had a central/peripheral index of grade 2 or above (*C/P* ratio grade 2–4: 0.44±0.21 vs. grade-0–1: 0.22±0.12, *P*=0.02).
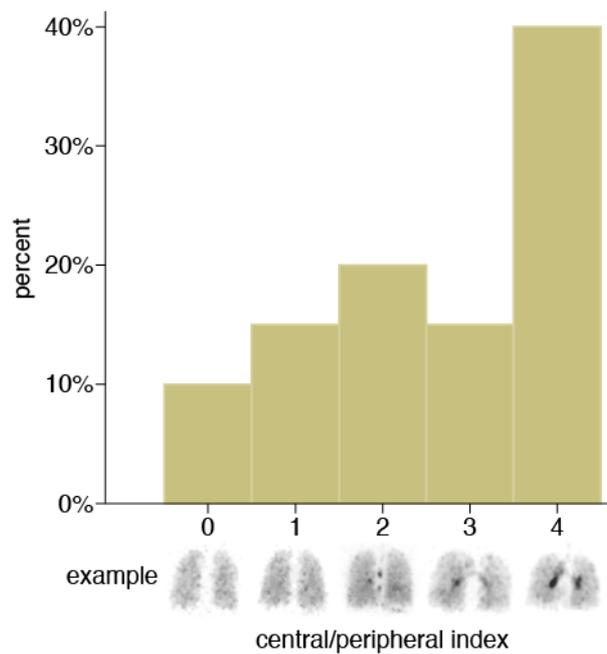
TABLES

Table 1. Peak expiratory flow rate at baseline and after inhalation (N=20)

Characteristics	Baseline	After inhalation	*P*-value
Peak expiratory flow rate [L/s]	8.1±1.7	8.0±1.3	0.9
Gender:			
Women (N=13)	7.1±0.7	7.1±0.6	0.8
Men (N=7)	9.8±1.2*	9.6±0.5*	0.6
Smoking status:			
Non-smoker (N=15)	8.1±1.8	8.0±1.4	0.7
Smoker (N=5)	8.1±1.4†	8.2±1.2†	1.0

*Significant difference vs. women (*P*=0.0005 at baseline; *P*<0.0001 after inhalation);

†No difference vs. non-smokers (*P*=0.9 at baseline; *P*<0.7 after inhalation).